Scanning tunneling microscopy of interface properties of Bi_2Se_3 on FeSe

Scanning tunneling microscopy of interface properties of Bi_2Se_3 on FeSe

Yilin Wang[1], Yeping Jiang[1,2], Mu Chen[1,2], Zhi Li[1], Canli Song[1,2], Lili Wang[1], Ke He[1], Xi Chen[2], Xucun Ma[1] and Qi-Kun Xue[1,2]

[1] State Key Laboratory for Surface Physics, Institute of Physics, Chinese Academy of Sciences, Beijing 100190, People's Republic of China
[2] State Key Laboratory of Low-Dimensional Quantum Physics, Department of Physics, Tsinghua University, Beijing 100084, People's Republic of China

E-mail: xcma@iphy.ac.cn

Abstract

We investigate the heteroepitaxial growth of Bi_2Se_3 films on FeSe substrates by low-temperature scanning tunneling microscopy/spectroscopy. The growth of Bi_2Se_3 on FeSe proceeds via van der Waals epitaxy with atomically flat morphology. A striped moiré pattern originating from the lattice mismatch between Bi_2Se_3 and FeSe is observed. Tunneling spectra reveal the spatially inhomogeneous electronic structure of the Bi_2Se_3 thin films, which can be ascribed to the charge transfer at the interface.

(Some figures may appear in colour only in the online journal)

1. Introduction

Heterostructures do play an important role in both fundamental and applied science [1, 2]. For instance, the topological insulator/superconductor heterostructure has been recently proposed as a prototype to detect Majorana fermions for quantum computation and has attracted great attention [3]. However, very little work has been done to realize such a heterostructure so far, except for a recent paper in which topological order and superconductivity were found to coexist in Bi_2Se_3 thin films grown on a $NbSe_2$ substrate [4]. In spite of a large number of superconductors and topological insulators, it is very challenging to make such a heterostructure with a sharp interface due to the following reason. For conventional semiconductor heterostructures, a high-quality interface is usually obtained when the substrate and epilayer are lattice-matched, AlGaAs/GaAs is one of the examples. On the other hand, when the substrate and epilayer have no dangling bonds on their surfaces, the heteroepitaxial growth proceeds via van der Waals interaction. In this case, lattice-match is not essential. This type of epitaxy is called van der Waals epitaxy (VDWE) [5–7]. VDWE has been successfully applied to grow layered material on other layered materials or passivated substrates [8–14], such as $MoS_2/MoSe_2$ [9, 8] and GaSe/Si [11]. Using VDWE, we have successfully prepared

high-quality Bi_2Se_3 films [15–17] and FeSe films [18, 19]. Bi_2Se_3 is one of the prototype topological insulators (TIs) and has a rhombohedral structure [20]. FeSe is the simplest among the newly discovered iron-based superconductors, it has a tetragonal structure [21]. Both Bi_2Se_3 and FeSe have a layered structure. Along the c direction, one unit cell contains five atomic layers (Se–Bi–Se–Bi–Se) called a quintuple layer (QL), while it contains three atomic layers (Se–Fe–Se) called a triple layer (TL) in the case of FeSe. Within a QL (TL), the chemical bond between Bi (Fe) and Se atoms is of covalent–ionic type; whereas between the adjacent QLs (TLs) the interaction is of van der Waals type. In the a–b plane, the atoms of Bi_2Se_3 and FeSe are arranged in hexagonal symmetry with a lattice constant of 0.414 nm and in square symmetry with a lattice constant of 0.378 nm, respectively. To date, the growth mechanism and particularly the interface property between Bi_2Se_3 and FeSe remain unexplored.

In this paper, we present a scanning tunneling microscopy/spectroscopy (STM/STS) study on the heteroepitaxial growth of Bi_2Se_3 on FeSe. Although their lattices have different symmetry and the lattice mismatch is as large as 9.5%, we find an atomically sharp interface can form between Bi_2Se_3 and FeSe. On the Bi_2Se_3 surface, a striped moiré pattern is observed and its periodicity varies with location, indicating the existence of strain at the interface. The dI/dV
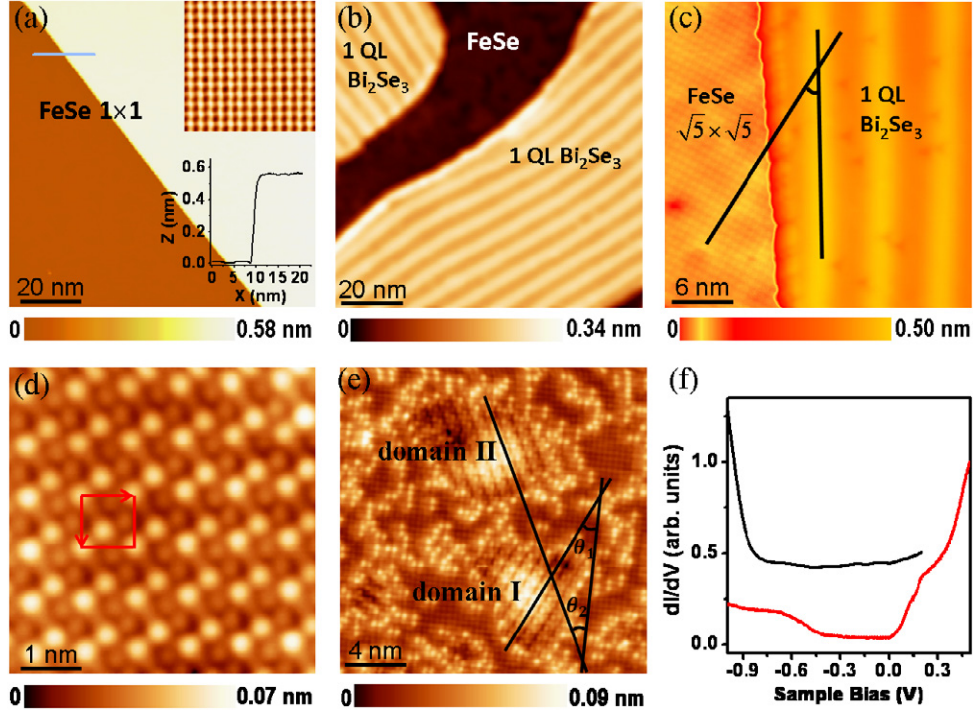
Figure 1. (a) STM topographic image of a 20 TL superconducting FeSe film (100×100 nm^2, $V = 2.5$ V, $I = 0.1$ nA). The upper inset shows the atomic-resolution image of FeSe film (5×5 nm^2, $V = 0.1$ V, $I = 0.1$ nA). The selenium atom spacing is about 0.38 nm. The lower inset shows the profile along the cyan line. (b) STM image showing the striped surface after depositing ~ 0.5 QL Bi$_2$Se$_3$ on FeSe (100×100 nm^2, $V = 5.0$ V, $I = 0.05$ nA). (c) High-resolution STM image of the interface between Bi$_2$Se$_3$ and FeSe (30×30 nm^2, $V = 0.5$ V, $I = 0.1$ nA). The superconducting FeSe 1×1 phase is changed to the semiconducting FeSe $\sqrt{5} \times \sqrt{5}$ phase. The angle between the stripes and one of lattice vectors of the FeSe $\sqrt{5} \times \sqrt{5}$ phase is $27 \pm 4°$. (d) The atomic-resolution image of FeSe $\sqrt{5} \times \sqrt{5}$ phase (5×5 nm^2, $V = 1$ mV, $I = 0.25$ nA). (e) STM topographic image of the FeSe surface at a Se doping level of 7.0% (20×20 nm^2, $V = 0.3$ V, $I = 0.1$ nA). The angle between lattice vectors of both domains I and II and the FeSe 1×1 phase is $\theta_1 = \theta_2 = 26.5°$. (f) d$I$/d$V$ curves taken on the FeSe $\sqrt{5} \times \sqrt{5}$ phase (bottom) and the first QL Bi$_2$Se$_3$ film (top), respectively. Set point: $V = 0.5$ V, $I = 0.1$ nA. Spectra are vertically displaced for clarity.

curves at different sites of the second QL Bi$_2$Se$_3$ films have an energy shift, suggesting the spatially inhomogeneous electronic properties of the Bi$_2$Se$_3$ thin films.

2. Experiment

The Bi$_2$Se$_3$/FeSe heterostructures were prepared by molecular beam epitaxy and characterized *in situ* by low-temperature STM (Unisoku). The base pressure of the system is better than 1.0×10^{-10} Torr. High-purity Bi (99.999%), Se (99.999%) and Fe (99.995%) were thermally evaporated from Knudsen cells. The FeSe film was prepared on bilayer graphene formed on 6H-SiC(0001). The Bi$_2$Se$_3$ film was then deposited on the FeSe film. For the growth of FeSe and Bi$_2$Se$_3$ films, the substrate temperatures were kept at $450\,°$C and $220\,°$C, respectively. The growth conditions of Bi$_2$Se$_3$ films on FeSe are the same as that on graphene. Details of the growth have been described elsewhere [15, 18, 19]. The STM measurements were performed in the constant current mode with electrochemically etched polycrystalline *W* tips at 4.8 K. The bias voltage was applied to the sample. The STS spectra were acquired using a standard lock-in technique.

3. Results and discussion

Figure 1(a) shows a typical STM topographic image of as-grown FeSe film with a nominal thickness of 20 TL on graphene on 6H-SiC(0001) [18]. The atomically flat film grows along the (001) direction with a step height of one TL (0.55 nm, the lower inset of figure 1(a)). The upper inset of figure 1(a) shows an atomically resolved STM image of FeSe film, which presents the square lattice structure of the Se-terminated (001) surface with a lattice constant $a = 0.38$ nm, matching well with that of superconducting β-FeSe [21]. A superconducting gap of 2.2 meV was observed on such a FeSe film [18, 19]. Figures 1(b) and (c) show the surface morphology of approximate 0.5 QL Bi$_2$Se$_3$ deposited on FeSe, shown in figure 1(a). The striped patterns running along two almost perpendicular orientations can be seen. They originate from the four-fold symmetry of FeSe(001). The striped moiré pattern results from the mismatch of the hexagonal Bi$_2$Se$_3$ lattice and the square FeSe lattice, as discussed below. As shown in figure 1(c), the interface between Bi$_2$Se$_3$ and FeSe is very sharp. Interestingly, the FeSe surface has been changed from the original 1×1 phase to the $\sqrt{5} \times \sqrt{5}$ phase with a lattice parameter of 0.85 nm (left part in figure 1(c)), due to the Se-rich condition for
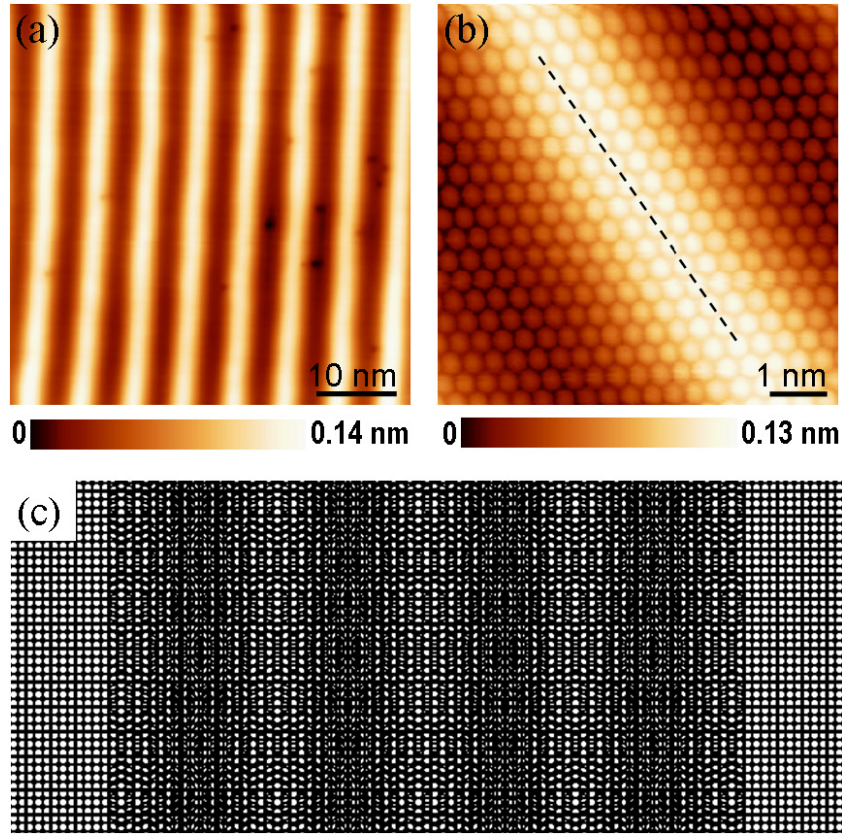
Figure 2. (a) High-resolution STM image of the striped moiré pattern in the first QL Bi_2Se_3 film (50×50 nm^2, $V = 2.5$ V, $I = 0.1$ nA). (b) The atomic-resolution image of the first QL Bi_2Se_3 film (7×7 nm^2, $V = 1$ mV, $I = 0.35$ nA). (c) Simulation of the striped moiré pattern with the FeSe 1×1 lattice and Bi_2Se_3 lattice rotated by 0°.

preparation of Bi_2Se_3 films [19], therefore, the actual interface for Bi_2Se_3/FeSe is the FeSe $\sqrt{5} \times \sqrt{5}$ phase. Figure 1(d) shows the high-resolution STM image of the $\sqrt{5} \times \sqrt{5}$ phase, in which the ordered bright dumbbell-like pairs and the FeSe 1×1 lattice can be clearly observed. The $\sqrt{5} \times \sqrt{5}$ phase is not a real lattice structure or reconstruction [18, 19]. It has an electronic origin of FeSe induced by extra Se atoms at substitutional, interstitial or intercalated sites. In fact, the FeSe 1×1 phase can be partially changed to the $\sqrt{5} \times \sqrt{5}$ phase if one changes the doping level of Se atoms by a certain amount, 7%, for example (more results can be found at [18, 19]). The random nucleation of Se atoms leads to two $\sqrt{5} \times \sqrt{5}$ domains, as shown in figure 1(e). Both domains I and II rotate $\theta_1 = \theta_2 = 26.5°$ with respect to the FeSe 1×1 phase lattice. These structural details enable us to analyze the epitaxial relationship between Bi_2Se_3 and FeSe. Figure 1(f) shows the dI/dV curves taken on the surface of the first QL Bi_2Se_3 film (top) and on the FeSe $\sqrt{5} \times \sqrt{5}$ phase (bottom), respectively. The FeSe $\sqrt{5} \times \sqrt{5}$ phase exhibits an asymmetric gap of $\sim$0.5 eV near E_F [19, 18] because the property of FeSe is very sensitive to the stoichiometry.

We now turn to discuss the properties of the striped patterns. Figure 2(a) shows a typical STM image of the striped patterns with a period of $\sim$6.4 nm. The striped patterns are not dependent on bias and exhibit similar features in both filled and empty states, except for a small contrast change. The atomically resolved image in figure 2(b) reveals a hexagonal

structure with a lattice constant $a = 0.41 \pm 0.01$ nm, which is almost the same as that of Bi_2Se_3. This indicates the heteroepitaxial Bi_2Se_3 film grows with its own lattice even at the first QL.

The similar striped patterns were also observed in the graphene on Cu (100) system [22]. If the hexagonal and square lattices overlap, a striped moiré pattern will be formed. We can reproduce the observed striped patterns by superimposing the lattice (0.414 nm) of Bi_2Se_3 on that (0.378 nm) of the FeSe 1×1 phase. As shown in figure 2(b), one of the close-packed directions of Bi_2Se_3 (dashed line) is along the stripes. The angle between the stripes and one of the lattice vectors of the FeSe $\sqrt{5} \times \sqrt{5}$ phase is $27 \pm 4°$ (figure 1(c)). The angle between the lattice vectors of the FeSe $\sqrt{5} \times \sqrt{5}$ phase and FeSe 1×1 phase is 26.5° (figure 1(e)). Therefore we deduce that one of lattice vectors of Bi_2Se_3 is parallel to that of the FeSe 1×1 phase. Figure 2(c) shows the simulated striped patterns. In this case, the periodicity of the striped patterns is $\sim$6.8 nm. If the epitaxial film is uniform, the formed moiré pattern should also be uniform. In fact, the periodicity of the striped patterns varies from 6.0 to 7.2 nm, which probably comes from lattice distortion in Bi_2Se_3 induced by interface strain [8, 22]. The minimum and maximum periods of striped patterns, 6.0 nm and 7.2 nm, correspond to lattice constants of 0.410 nm and 0.415 nm for Bi_2Se_3, respectively. The non-uniform striped patterns might also be induced by a small rotation of the
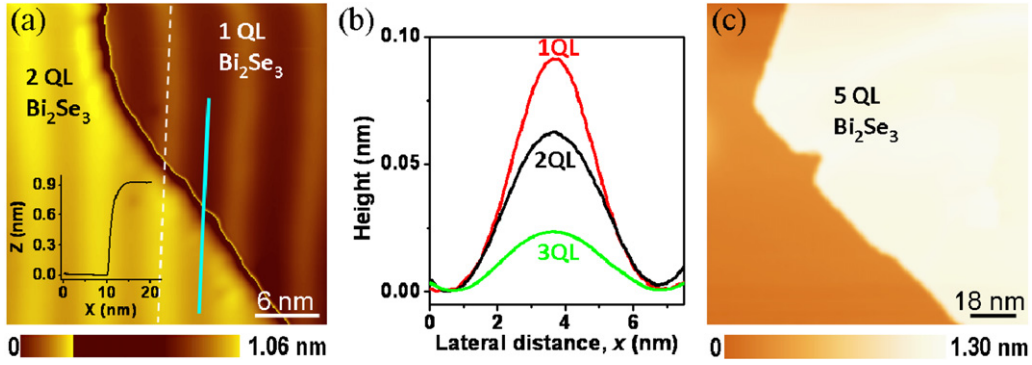
Figure 3. (a) STM topographic image of the striped moiré patterns in the first and the second QL Bi$_2$Se$_3$ films (30×30 nm^2, $V = 0.5$ V, $I = 0.1$ nA). The inset shows the profile along the cyan line. (b) Height profiles of the striped patterns in the first (top), the second (medium), and the third (bottom) QL Bi$_2$Se$_3$ films, respectively. (c) STM image of the fifth QL Bi$_2$Se$_3$ film (90×90 nm^2, $V = 4.0$ V, $I = 0.05$ nA).

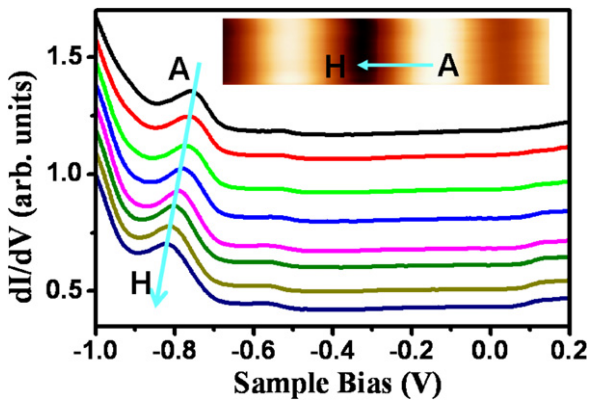**Figure 4.** STS spectra obtained along the line shown in the inset. Set point: $V = 0.5$ V, $I = 0.1$ nA. The curves are offset vertically for clarity. The inset shows the STM image of the second QL Bi$_2$Se$_3$ film (15×3 nm^2, $V = 0.5$ V, $I = 0.1$ nA).

Bi$_2$Se$_3$ lattice with respect to that of FeSe. The appearance of the moiré pattern indicates the interaction between Bi$_2$Se$_3$ and FeSe is very weak. The weak van der Waals interaction could introduce strain at the interface [13].

The Bi$_2$Se$_3$ films grow on FeSe by the layer-by-layer mode. The second QL Bi$_2$Se$_3$ films start to grow only after completion of the first QL. Interestingly, we observed similar striped patterns on the second QL Bi$_2$Se$_3$ films with different contrast, as shown in figure 3(a). The stripes in the first and the second QL films are located at the same place (the dashed line in figure 3(a)). The height profiles of the striped patterns in the first, the second, and the third QL Bi$_2$Se$_3$ films are shown in figure 3(b), in which the amplitude of stripes gradually decreases from 0.09 to 0.06 nm, and then to 0.02 nm. The striped patterns disappear at the fifth QL (figure 3(c)). The striped patterns in the second to the fourth QL Bi$_2$Se$_3$ films reflect the subsurface structures, which are usually not observed by STM. However, it has been theoretically demonstrated that the laterally nanoscale waves decay rather slowly and can propagate through many layers of epilayers [23].

We also studied the electronic structure of the second QL Bi$_2$Se$_3$ film and found its electronic structure is not homogeneous because of the moiré pattern. We choose the second QL Bi$_2$Se$_3$ film because there is no obvious feature in the dI/dV curve of the first QL Bi$_2$Se$_3$ film (figure 1(f)). Figure 4 shows the dI/dV curves on eight evenly separated (0.5 nm) points (A through H) along the line shown in the STM image of the second QL Bi$_2$Se$_3$ films (inset of figure 4). The STS spectra on all points are quite similar, except for the peaks at negative bias, which correspond to the highest occupied state (HOS) of Bi$_2$Se$_3$. The HOS is located at -0.76 V for the stripe peak and gradually shifts to -0.82 V for the valley. A similar phenomenon was also observed in other systems, such as graphite/Pt(111) [24], graphene/Ru(0001) [25, 26], and NaCl/Ag(100) [27]. The periodically modulated electronic properties can be interpreted as the interaction [24, 25] and charge transfer [27, 26] between the adsorbate and substrate. In fact, the charge transfer mechanism plays an important role in tuning the chemical potentials of materials. The HOS position of the second QL Bi$_2$Se$_3$ films grown on FeSe is different from that grown on graphene/SiC(0001) (data not shown, the HOS position is -0.62 V). It is caused by different substrate doping effects [15]. When two materials with different individual Fermi levels are placed in contact, electrons are transferred from the material with the higher Fermi level to the other material until their Fermi levels are equal. The work functions of epitaxial graphene (EG), FeSe and Bi$_2$Se$_3$ are ~ 4.0 eV [28], ~ 2.5 eV [29] and ~ 5.5 eV [30], respectively. The Fermi levels of EG and FeSe are higher than that of Bi$_2$Se$_3$, therefore charge transfer occurs from EG and FeSe to Bi$_2$Se$_3$. The band structure of Bi$_2$Se$_3$ will be shifted downwards (towards negative direction) once it is electron doped [31]. The more doped electrons, the more the shift of the band structure. The Fermi level of FeSe is higher than that of EG and the amount of electrons transferred from FeSe to Bi$_2$Se$_3$ is larger than that from EG to Bi$_2$Se$_3$, therefore the HOS position of Bi$_2$Se$_3$ on FeSe is more negative than that of Bi$_2$Se$_3$ on EG. Charge transfer is also expected to decay exponentially with distance. In stripe patterns, the distance between the substrate and the valley sites is smaller than that between the substrate and the peak sites because the occurrence of the moiré pattern is also accompanied with lattice displacement [32]. Therefore the charge transfer

amount in the valley sites is larger than that in the peak sites, which leads to the HOS position at the valley shifting to a more negative value, as observed here.

4. Summary

In summary, we found an atomically sharp interface is formed between Bi_2Se_3 and FeSe. The Bi_2Se_3 film is fully relaxed even at the first QL, leading to a striped moiré pattern. The electronic structure of epitaxial Bi_2Se_3 thin films is periodically modulated by the moiré pattern due to a different charge transfer amount at different regions of the pattern. Our results provide very useful information for the study of van der Waals epitaxy and also for constructing heterostructures composed of this kind of material.

Acknowledgments

References

[1] Stormer H L 1999 *Rev. Mod. Phys.* **71** 875
[2] Alferov Z I 2001 *Rev. Mod. Phys.* **73** 767
[3] Fu L and Kane C L 2008 *Phys. Rev. Lett.* **100** 096407
[4] Wang M -X *et al* 2012 *Science* **336** 52
[5] Koma A, Sunouchi K and Miyajima T 1985 *J. Vac. Sci. Technol.* B **3** 724
[6] Koma A 1992 *Surf. Sci.* **267** 29
[7] Koma A 1999 *J. Cryst. Growth* **201** 236
[8] Mori T, Abe H, Saiki K and Koma A 1993 *Japan. J. Appl. Phys.* **32** 2945
[9] Murata H and Koma A 1999 *Phys. Rev.* B **59** 10327
[10] Tiefenbacher S, Pettenkofer C and Jaegermann W 2000 *Surf. Sci.* **450** 181
[11] Jaegermann W, Rudolph R, Klein A and Pettenkofer C 2000 *Thin Solid Films* **380** 276
[12] Ohuchi F S, Parkinson B A, Ueno K and Koma A 1990 *J. Appl. Phys.* **68** 2168
[13] Parkinson B A, Ohuchi F S, Ueno K and Koma A 1991 *Appl. Phys. Lett.* **58** 472
[14] Koma A and Yoshimura K 1986 *Surf. Sci.* **174** 556
[15] Song C -L *et al* 2010 *Appl. Phys. Lett.* **97** 143118
[16] Zhang Y *et al* 2010 *Nature Phys.* **6** 584
[17] Cheng P *et al* 2010 *Phys. Rev. Lett.* **105** 076801
[18] Song C L *et al* 2011 *Science* **332** 1410
[19] Song C -L, Wang Y -L, Jiang Y -P, Li Z, Wang L, He K, Chen X, Ma X -C and Xue Q -K 2011 *Phys. Rev.* B **84** 020503
[20] Zhang H J, Liu C X, Qi X L, Dai X, Fang Z and Zhang S C 2009 *Nature Phys.* **5** 438
[21] Hsu F C *et al* 2008 *Proc. Natl Acad. Sci. USA* **105** 14262
[22] Cho J *et al* 2011 *ACS Nano* **5** 3607
[23] Kobayashi K 1996 *Phys. Rev.* B **53** 11091
[24] Sasaki M, Yamada Y, Ogiwara Y, Yagyu S and Yamamoto S 2000 *Phys. Rev.* B **61** 15653
[25] Gyamfi M, Eelbo T, Wasacuteniowska M and Wiesendanger R 2011 *Phys. Rev.* B **83** 153418
[26] Feng W, Lei S, Li Q and Zhao A 2011 *J. Phys. Chem.* C **115** 24858
[27] Pivetta M, Patthey F, Stengel M, Baldereschi A and Schneider W D 2005 *Phys. Rev.* B **72** 115404
[28] Chen W, Chen S, Qi D C, Gao X Y and Wee A T S 2007 *J. Am. Chem. Soc.* **129** 10418
[29] Ukita R, Sugimoto A and Ekino T 2012 *Physica* C at press
[30] Wu G, Chen H, Sun Y, Li X, Cui P, Franchini C, Wang J, Chen X -Q and Zhang Z 2012 arXiv:1203.6718
[31] Wang Y L *et al* 2011 *Phys. Rev.* B **84** 075335
[32] Kobayashi K and Yamauchi J 1996 *Surf. Sci.* **357** 317